Journal of Materials and Construction
ISSN 2734-9438
Website: www. jomc.vn

Evaluation of the effectiveness of molybdate-based coating on reinforcing steel during the pre-construction phase of offshore projects

Le Van Toan[2], Nguyen Quy Thanh[1], Dang Minh Duc[3], Dang Thi Thu Hien[1,*]

[1] Institute of Techniques for Special Engineering, Le Quy Don Technical University

[2] Faculty of Physics and Chemical Engineering, Le Quy Don Technical University

[3] School of Materials Science and Engineering, Hanoi University of Science and Technology

KEYWORDS

Ammonium heptamolybdate (AHM)
Reinforcing steel
Corrosion inhibition
Offshore construction
Electrochemical testing

ABSTRACT

The corrosion behavior of carbon steel in 3.5 wt.% NaCl solution and the inhibition performance of ammonium heptamolybdate (AHM)/sodium carbonate (Na_2CO_3) were investigated using electrochemical techniques (Tafel, EIS), gravimetric measurements, and SEM/EDS analyses. The unprotected steel showed rapid corrosion, as indicated by high Icorr, low Rcorr, and severe surface damage. The addition of AHM/Na_2CO_3 significantly reduced corrosion, with the In3 system (1.5 g/L AHM + 1.5 g/L Na_2CO_3) exhibited the best performance In3 achieved the lowest Icorr, the highest resistance, and an inhibition efficiency above 95%. Gravimetric measurements confirmed long-term stability, while SEM/EDS revealed a compact and adherent protective film that effectively blocked chloride penetration. These results highlight In3 as an highly effective and sustainable corrosion inhibitor for carbon steel in chloride environments, suitable for protecting steel during transportation to offshore construction sites.

1. Introduction

The durability of reinforced concrete structures in offshore and marine environments depends heavily on the corrosion resistance of reinforcing steel. Chloride ingress, particularly from seawater exposure, disrupts the passive oxide film on steel and accelerates corrosion, thereby compromising structural integrity and reducing service life [1]. Corrosion-induced deterioration of marine infrastructure such as bridges, ports, and offshore platforms contributes significantly to global maintenance costs [2].

Conventional corrosion protection methods, including increased concrete cover, low-permeability concrete, epoxy-coated rebars, stainless steel, and cathodic protection, These methods offer advantages in corrosion resistance but are limited by high cost, difficult application procedures, and vulnerability to mechanical damage) [3]. Hence, strategies that can be applied during the pre-construction phase—when rebars are exposed to aggressive saline conditions before concrete casting—are increasingly important in construction practice) [4].

Inorganic corrosion inhibitors have recently become recognized as a potentially effective and somewhat more environmentally friendly alternative to organic coatings, with molybdate-based systems being particularly attractive [5] [6]. Molybdate ions act primarily as anodic inhibitors, stabilizing and thickening passive films, thereby delaying the onset of localized corrosion in chloride-rich media [7] [8]. Compared with chromates, molybdates are considered more environmentally acceptable and less toxic, while still providing strong passivating effects [9] [10].

Several studies have demonstrated the effectiveness of molybdate on steel corrosion in simulated concrete pore solutions and chloride-contaminated mortars. Shi et al. (2022) showed that molybdate admixtures shifted corrosion potentials to more noble values and increased polarization resistance, significantly delaying corrosion initiation in reinforced mortars exposed to 3.5 wt.% NaCl [1]. Similarly, Wu et al. (2021) reported both beneficial and detrimental effects of molybdate: at low concentrations, molybdate enhanced passivity, while excessive dosages altered solution chemistry and potentially interfered with cement hydration [11]. Other works explored synergistic effects, such as combining molybdate with phytate or lignosulfonates, which yielded more compact and adherent films [12] [13].

Despite these promising findings, few studies have focused on the application of molybdate-based pretreatments for reinforcing steel before construction. In this scenario, rebars are temporarily exposed to marine environments during handling, storage, and transport, creating a vulnerable period for corrosion initiation [14]. Therefore, understanding the protective efficiency of molybdate-based surface treatments under these conditions is essential for extending the durability of offshore structures.

In this study, we investigate the corrosion protection effectiveness of molybdate-based coatings formed from ammonium molybdate (AHM) and sodium carbonate at varying concentrations. Electrochemical techniques (EIS, Tafel) and gravimetric weight loss tests in 3.5 wt.% NaCl were combined with surface characterization (SEM/EDS) to elucidate inhibitor adsorption and protective film formation. The outcomes are expected to assess the applicability of

*Corresponding author: thuhien118v2@gmail.com
Received 04/10/2025, Revised 25/11/2025, Accepted 26/11/2025
Link DOI: https://doi.org/10.54772/jomc.v15i02.1123

molybdate pretreatments as a practical and sustainable corrosion control measure for reinforcing steel in offshore construction [15].

2. Experiment

2.1. Materials and Surface Treatment

Commercial reinforcing steel bars (diameter 10 mm) were cut into coupons with a thickness of 3 mm. Prior to treatment, the specimens were sequentially ground with SiC papers up to 1200 grit, rinsed with deionized (DI) water, ultrasonically cleaned in ethanol for 10 min, and dried under warm airflow.

Four inhibitor solutions (In1–In4) were prepared using ammonium molybdate ($(NH_4)_6Mo_7O_{24}{\cdot}4H_2O$, AHM) and sodium carbonate (Na_2CO_3) in DI water to investigate the effect of inhibitor concentration on steel corrosion in 3.5 wt.% NaCl. The compositions were: In1 – 0.5 g/L AHM + 0.5 g/L Na_2CO_3; In2 – 1.0 g/L AHM + 1.0 g/L Na_2CO_3; In3 – 1.5 g/L AHM + 1.5 g/L Na_2CO_3; and In4 – 2.0 g/L AHM + 2.0 g/L Na_2CO_3. Steel specimens were immersed in the corresponding inhibitor solution at room temperature for 3 h, rinsed with DI water, and dried in a desiccator. Untreated steel was used as the control referred to as Blank.

2.2. Electrochemical and Gravimetric Evaluation

Electrochemical measurements were conducted in 3.5 wt.% NaCl using a conventional three-electrode cell. The steel sample served as the working electrode, a saturated calomel electrode (SCE) as the reference, and a platinum plate as the counter electrode. Open-circuit potential (OCP) was monitored for 1 h before testing. Electrochemical impedance spectroscopy (EIS) was performed over a frequency range of 100 kHz to 10 mHz with a 10 mV AC perturbation. Potentiodynamic polarization (Tafel) scans were conducted at 1 mV/s within ±100 mV with respect to OCP Weight loss tests were performed by immersing the specimens in 3.5 wt.% NaCl for 1, 3, 5, and 7 days, followed by cleaning, drying, and gravimetric analysis.

2.3. Surface Characterization

The surface morphology and elemental composition of the specimens were examined using scanning electron microscopy (SEM) coupled with energy-dispersive X-ray spectroscopy (EDS) to evaluate inhibitor adsorption and the formation of protective films. Representative SEM and EDS images were collected to correlate surface features with corrosion performance.

3. Results and discussion

3.1. Electrochemical Characteristics

Figure 1 presents the Tafel polarization curves of carbon steel in 3.5 wt.% NaCl solution in the absence (Blank) and presence of AHM/Na_2CO_3 inhibitors (In1–In4). The corresponding electrochemical parameters are summarized in Table 1, which shows a significant reduction in corrosion current density and an improvement in inhibition efficiency, confirming the notable effect of the inhibitor solutions on the corrosion behavior of carbon steel.

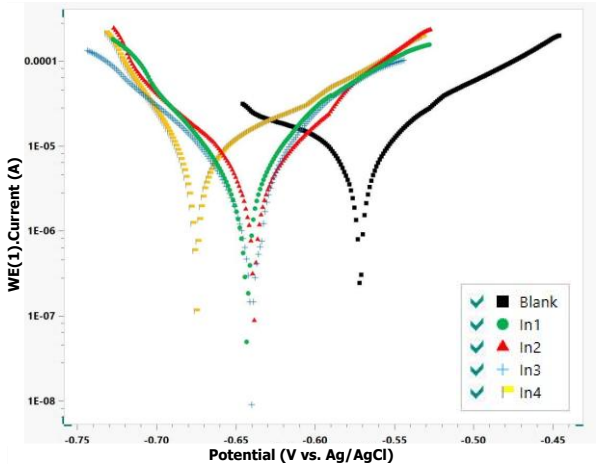

Figure 1. Tafel polarization curves of carbon steel in 3.5 wt.% NaCl solution in the absence (Blank) and presence of AHM/Na_2CO_3 inhibitors (In1–In4).

For the uninhibited sample (Blank), the corrosion current density (I_{corr}) reached the highest value of 1.1629×10^{-5} A/cm^2, while the polarization resistance (R_{corr}) was only 1929.1 Ω·cm^2. The corresponding corrosion rate was also high, at 0.135 mm/year. These findings confirm that in chloride-containing environments, steel undergoes severe corrosion with almost no inherent surface protection

Table 1. Results of Tafel Polarization Curve Analysis.

Samples	E_{corr} (V)	I_{corr} (A/cm^2)	R_{corr} (Ωcm^2)	Corrosion rate (mm/year)	H (%)
In1	-0.63963	7.2701×10^{-6}	2708.7	0.084478	37.48
In2	-0.65282	4.1861×10^{-6}	4141.2	0.048642	64.00
In3	-0.6582	5.5142×10^{-7}	6393.8	0.0064075	95.26
In4	-0.67742	6.5278×10^{-6}	1786.3	0.075853	43.87
Blank	-0.57196	1.1629×10^{-5}	1929.1	0.13513	-

Upon the addition of inhibitors, a a significant improvement was recorded. For In1 and In2, Icorr decreased to 7.27 × 10^{-6} and 4.19 × 10^{-6} A/cm^2, respectively, while R_{corr} increased to 2708.7 and 4141.2 Ω·cm^2. The inhibition efficiency (H) values were 37.48 % and 64.0 %, respectively. This indicates that as the concentration of AHM/Na_2CO_3 increases, MoO_4^{2-} and CO_3^{2-} ions begin to adsorb on the steel surface, forming an initial protective film that suppresses both iron dissolution and the oxygen reduction reaction.

In particular, In3 exhibited excellent inhibition efficiency. Icorr sharply decreased to 5.51 × 10^{-7} A/cm^2, R_{corr} increased to 6393.8 Ω·cm^2, and the corrosion rate dropped to only 0.0064 mm/year. The inhibition efficiency reached as high as 95.26 %. At this optimal concentration (1.5 g/L AHM + 1.5 g/L Na_2CO_3), the synergistic interaction between MoO_4^{2-} and CO_3^{2-} ions facilitated the formation of a robust, continuous, and stable protective film on the steel surface, acting as an effective barrier against the penetration of chloride ions and oxygen.

However, at higher inhibitor concentrations (In4), the inhibition efficiency decreased significantly to 43.87 %. This decline may be attributed to an “overdose” effect, in which excessive concentrations of AHM and Na_2CO_3 destabilize the protective layer, generate defects, or increase the conductivity of the solution, thereby increasing Icorr.

Overall, the electrochemical results confirm that the AHM/Na_2CO_3 system provides substantial protection for steel in chloride environments, with the optimal condition being In3, achieving an inhibition efficiency exceeding 95 %. Together with EIS and SEM/EDS analyses, the proposed protection mechanism is further supported by the presence of a Mo- and C-rich film tightly covering the steel surface, effectively acting as a barrier layer that prevents corrosion processes.

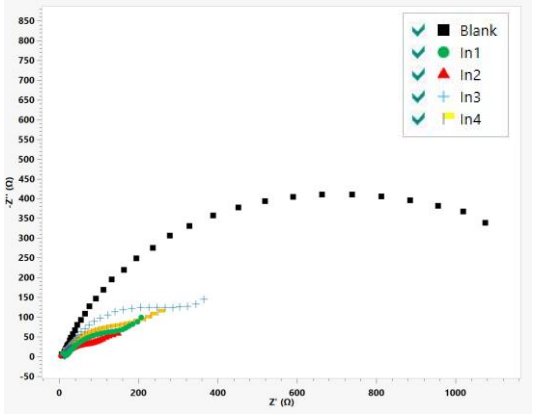

Figure 2. EIS spectra of carbon steel in 3.5 wt.% NaCl solution in the absence (Blank) and presence of AHM/Na_2CO_3 inhibitors (In1–In4).

The Nyquist and Bode plots demonstrate significant differences in impedance response between the uninhibited sample and inhibited systems. The presence of AHM/Na_2CO_3 inhibitors increases the diameter of the capacitive semicircle, suggesting enhanced charge transfer resistance. The equivalent circuit model was employed to fit the experimental data, confirming the improvement of corrosion resistance in the presence of In1–In4.

Electrochemical investigations combining potentiodynamic polarization (Tafel), electrochemical impedance spectroscopy, and equivalent circuit fitting (Figure 4) provided a comprehensive understanding of the inhibition performance of the investigated systems. The Nyquist (Figure 2) and Bode (Figure 3) plots for the blank steel substrate showed the highest charge transfer resistance (R_p = 1330 Ω·cm^2, Table 2), indicating of a thin native oxide film. However, the constant phase element (CPE) parameters, namely a high interfacial capacitance (Y_0 = 1.77 mMho·s^n) and a low exponent (n = 0.726), suggested surface inhomogeneity and a poorly protective oxide layer. These findings agreed with the Tafel analysis, which revealed a high corrosion current density for the blank.

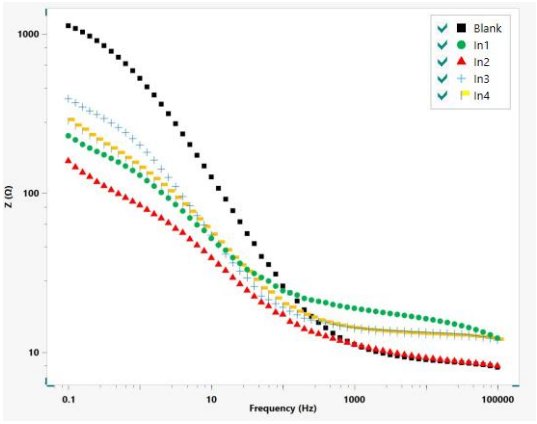

Figure 3. Bode plots of carbon steel in 3.5 wt.% NaCl solution in the absence (Blank) and presence of AHM/Na_2CO_3 inhibitors (In1–In4).

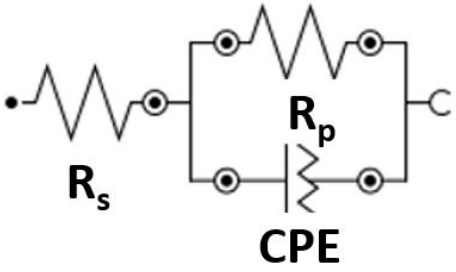

Figure 4. Equivalent circuit model used for fitting the EIS data of the samples.

The Bode plots (Figure 3) further supported these results. At low frequencies, In3 maintained a higher |Z| value and broader phase angle than In1 and In2, demonstrating enhanced charge-transfer resistance and superior barrier properties. Although In4 displayed a relatively high Rp (1786 Ω·cm^2, Table 2), its high capacitance and moderate n value (0.456) suggested a porous, defect-prone film to defects, which is consistent with its lower inhibition efficiency observed in Tafel analysis.

Taken together, the integrated electrochemical results (Figures 2–4 and Table 2) confirmed that In3 provides the most effective corrosion inhibition by establishing a dense and homogeneous surface film that retards charge transfer and suppresses the corrosion process.

In the presence of inhibitors, R_p values decreased for In1 (302 Ω·cm^2) and In2 (258 Ω·cm^2), while their low CPE exponents (n = 0.603 and 0.450, respectively; Table 2) indicated irregular adsorption and the formation of non-uniform protective films. This was consistent with their relatively high corrosion current densities and low inhibition efficiencies from Tafel results. In contrast, the In3 system exhibited a more favorable electrochemical response. Although its R_p (435 Ω·cm^2) was lower than that of the blank, the reduced interfacial capacitance (Y_0 = 1.09 mMho·s^n) and the higher exponent (n = 0.805) indicated the formation of a compact, stable film. This interpretation is well supported by polarization data, where In3 achieved the lowest Icorr (5.51×10^{-7} A·cm^{-2}) and the highest inhibition efficiency (95.26 %).

The equivalent circuit model (Figure 4), consisting of R_s, R_p, and a constant phase element (CPE), accurately described the corrosion system with adsorbed films. The fitted parameters further emphasize the superior performance of In3, while In1, In2, and In4 exhibit non-uniform or unstable films that permitted chloride ion penetration. Overall, the EIS results confirmed that the AHM/Na_2CO_3 system significantly enhances the corrosion resistance of carbon steel in chloride environments, with In3 at the optimal concentration providing the most effective and stable protection.

3.2. Gravimetric measurements

Results of gravimetric measurements (Tables 3–6) provided further confirmation of the inhibitory performance of the AHM/Na_2CO_3 systems. The Blank sample consistently exhibited the highest mass reduction at all immersion times, reflecting the severe corrosion of steel when directly exposed to 3.5 wt.% NaCl solution without inhibitors. The presence of AHM/Na_2CO_3 solutions significantly reduced the mass loss, among which In3 demonstrated higher inhibition efficiency compared to the other systems. After 1 day (Table 3), the inhibition efficiency of In3 reached 57.3 %, markedly higher than those of In1, In2, and In4.

With prolonged immersion, the efficiency of In3 continued to increase steadily, reaching 60.7 % after 3 days (Table 4) and increasing to 90.6 % after 5 days (Table 5), then maintaining a very high level of 92.1 % at day 7 (Table 6). This progression indicates that In3 not only provides an immediate protective film at the early stage but also develops into a durable anti-corrosion barrier over time. In contrast, In1, In2, and In4 exhibited only moderate inhibition efficiencies, which tended to decline after 5–7 days, suggesting the formation of less stable protective films.

Table 2. Equivalent circuit parameters obtained from EIS fitting.

Sample	R_s (Ω)	R_p (Ω)	Y_o (mMho·s^n)	n
In1	5.94	302	4.55	0.603
In2	4.85	258	6.63	0.450
In3	4.55	435	1.09	0.805
In4	12.9	492	3.30	0.456
Blank	4.49	1330	1.94	0.726

Table 3. Weight loss and inhibition efficiency of the samples after 1 day immersion.

Inhibitions	Initial Weight W1 (g)	Final Weight W2 (g)	Weight Loss W1 - W2 (mg)	Inhibition Efficiency (IE %)
In1	2.6304	2.6260	4.4	50.6
In2	2.6116	2.6070	4.6	48.3
In3	2.6310	2.6272	3.8	57.3
In4	2.4871	2.4825	4.6	48.3
Blank	2.6271	2.6182	8.9	—

Table 4. Weight loss and inhibition efficiency of the samples after 3 days immersion.

Inhibitions	Initial Weight W1 (g)	Final Weight W2 (g)	Weight Loss W1 - W2 (mg)	Inhibition Efficiency (IE %)
In1	2.6187	2.6138	4.9	58.1
In2	2.6428	2.6380	4.8	59.0
In3	2.6420	2.6374	4.6	60.7
In4	2.6121	2.6067	5.4	53.8
Blank	2.6251	2.6134	11.7	—

Table 5. Weight loss and inhibition efficiency of the samples after 5 days immersion.

Inhibitions	Initial Weight W1 (g)	Final Weight W2 (g)	Weight Loss W1 - W2 (mg)	Inhibition Efficiency (IE %)
In1	2.6150	2.6055	9.5	40.6
In2	2.6340	2.6280	6.0	62.5
In3	2.4900	2.4885	1.5	90.6
In4	2.6285	2.6160	12.5	21.9
Blank	2.6280	2.6120	16.0	—

Table 6. Weight loss and inhibition efficiency of the samples after 7 days immersion.

Inhibitions	Initial Weight W1 (g)	Final Weight W2 (g)	Weight Loss W1 - W2 (mg)	Inhibition Efficiency (IE %)
In1	2.6155	2.6035	12.0	36.8
In2	2.6350	2.6280	7.0	63.2
In3	2.4920	2.4905	1.5	92.1
In4	2.6310	2.6159	14.9	21.1
Blank	2.6290	2.6120	16.0	—

The superior protection mechanism of In3 can be attributed to the synergistic and well-balanced interaction between MoO_4^{2-} and CO_3^{2-} ions at the optimal concentration. Such cooperative adsorption promotes the formation of a strongly adherent film on the steel surface, sealing defects and restricting chloride ion penetration. Combined with electrochemical and surface analysis results, these findings confirmed that In3 is the most effective inhibitor solution, providing durable and efficient protection of steel in chloride environments.

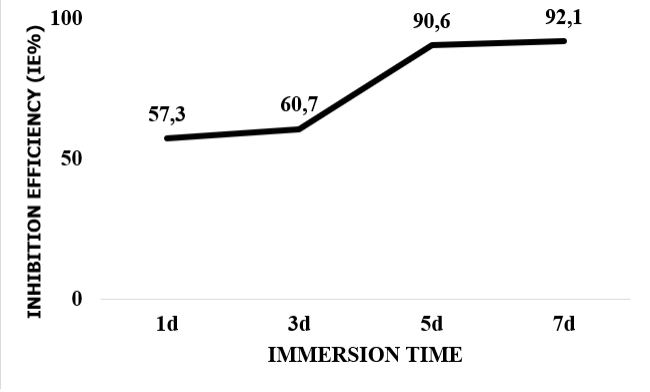

Figure 5. Inhibition efficiency as a function of immersion time in 3.5 % NaCl solution.

Figure 6 shows the surface morphologies of the steel specimens after 5 days of immersion in 3.5 % NaCl. The blank specimen (Figure 6a) exhibited severe surface degradation, with extensive rust layers and non-uniform corrosion attack, indicating aggressive chloride-induced corrosion in the absence of inhibitors.

By contrast, the inhibited samples display markedly improved surface conditions. In1 (Figure 6b) and In4 (Figure 6e) still reveal localized rust patches and areas of pitting, reflecting only partial protective ability. In2 (Figure 6c) presents a relatively more compact surface, although some scattered corrosion spots remain visible. Notably, In3 (Figure 6d) shows the most uniform and intact surface morphology, with minimal rust formation, confirming its more effective inhibition compared to the other formulations.

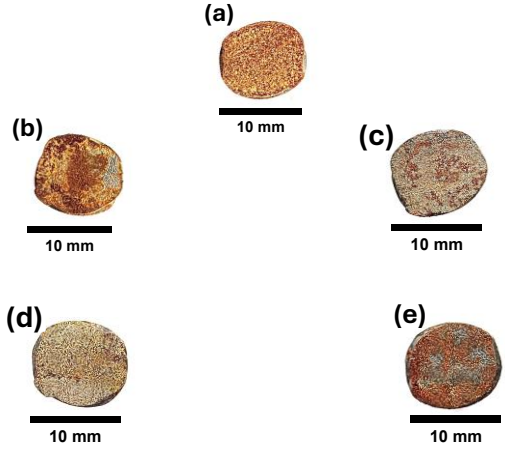

Figure 6. Surface morphologies of the steel specimens after 5 days of immersion in 3.5 % NaCl (a) Blank, (b) In1, (c) In2, (d) In3, and (e) In4.

These visual observations are consistent with the electrochemical results (Tables 3–6 and Figure 5), further verifying the protective role of the inhibitors, especially In3, in mitigating chloride-induced corrosion over prolonged immersion.

3.3. Surface Morphology

Figures 7 and 8 presented SEM images of the steel surface after immersion in 3.5 wt.% NaCl solution: (a) Blank and (b) with the In3 inhibitor solution. The images, captured at two different magnifications

(100× and 5000×), clearly highlight the differences in corrosion product morphology and protective film characteristics.

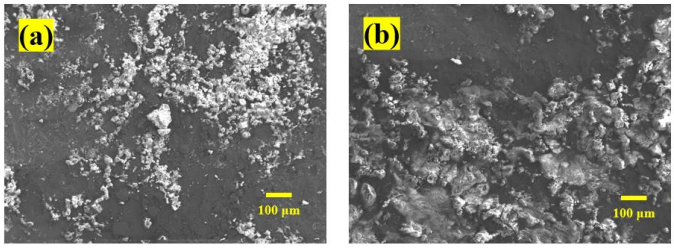

Figure 7. SEM images of (a) Blank and (b) In3 at 100× magnification.

Overall, comparison of SEM images at both magnifications (100× and 5000×) revealed pronounced differences between the Blank and In3 samples, fully consistent with the electrochemical results (lowest I_{corr}, highest R_{corr}, and inhibition efficiency ≈95 %). At low magnification (100×), the Blank surface showed numerous scattered and rough corrosion products with signs of localized pitting, whereas the In3 surface appeared more uniformly covered, with compact and adherent deposits, suggesting the formation of a more stable protective film.

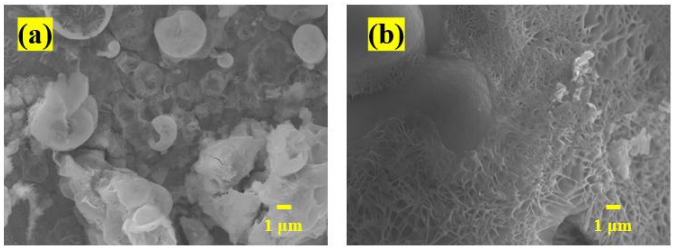

Figure 8. SEM images of (a) Blank and (b) In3 at 5000× magnification.

At higher magnification (5000×), the Blank surface exhibits porous, granular corrosion products with many voids that facilitate ion and electrolyte penetration, in line with its high Icorr and low Rcorr. In contrast, the In3 sample shows a fine and continuous network-like structure covering the surface, effectively sealing microdefects, limiting Cl^-/O_2 diffusion, and reducing the active electrochemical area. This mechanism explains why the Icorr of In3 decreased to 5.5142×10^{-7} A/cm^2, R_{corr} increased to 6393.8 Ω·cm^2, and the corrosion rate dropped to only ~0.0064 mm·y^{-1}. Thus, the combined SEM observations and electrochemical data confirm that the In3 inhibitor forms a continuous, effective protective film that significantly enhances the corrosion resistance of steel compared to the Blank.

3.4. Surface Chemical Composition

Figure 9 (a) shows the morphology and elemental composition of the steel sample after immersion in 3.5 wt.% NaCl solution for 7 days. The surface exhibits severe localized corrosion with numerous pits, indicating chloride-induced attack. The EDS spectrum reveals dominant Fe and O peaks together with detectable Cl, suggesting the formation of porous corrosion products mainly consisting of iron oxides/hydroxides (FeOOH, Fe_2O_3) and chloride-containing phases (e.g., FeOCl). [22]. Such deposits are loosely adherent and unable to provide effective protection against further corrosion.

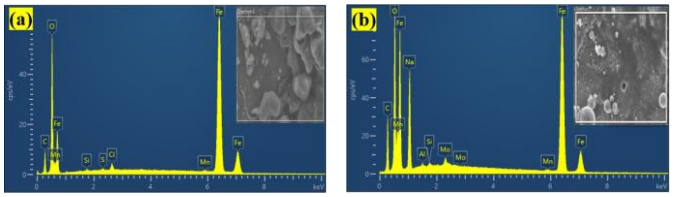

Figure 9. SEM–EDS images of (a) Blank and (b) In3.

In contrast, Figure 9 (b) corresponds to the steel sample pre-immersed in the In3 inhibitor solution (ammonium molybdate + Na_2CO_3) prior to exposure to NaCl. The SEM image displays a more compact morphology with particle-like deposits covering the surface. The EDS spectrum confirms the presence of Mo and Na in addition to Fe and O, indicating the incorporation of molybdate-derived compounds into the passive layer. The detected Mo species are most likely associated with iron molybdate phases ($Fe_2(MoO_4)_3$ or $FeMoO_4$) [25, 26], which are known to stabilize the passive film. The alkaline medium provided by Na_2CO_3 further promotes the precipitation of protective iron oxides/hydroxides in synergy with molybdate ions. As a result, a dense and adherent protective layer enriched with Mo–O compounds is formed, effectively hindering Cl^- ingress and mitigating localized corrosion.

4. Conclusion

Carbon steel in 3.5 wt.% NaCl is highly susceptible to corrosion, showing high corrosion current, low polarization resistance, rapid corrosion rate, and severe surface damage. The addition of AHM/Na_2CO_3 inhibitors markedly improves corrosion resistance, with In3 (1.5 g/L AHM + 1.5 g/L Na_2CO_3) exhibiting the lowest I_{corr}, highest R_p, and inhibition efficiency above 95 %, increasing from ~57 % after 1 day to over 92 % after 7 days. SEM/EDS analyses showed that In3 forms a uniform, well-adhered protective layer, effectively blocking chloride and oxygen penetration, while In1, In2, and In4 provide moderate and less stable protection. These results demonstrated that the AHM/Na_2CO_3 system, particularly In3, substantially enhances the corrosion resistance of carbon steel in chloride-containing environments.

References

[1]. J. Shi, M. Wu, and J. Ming, "In-depth insight into the role of molybdate in corrosion resistance of reinforcing steel in chloride-contaminated mortars," *Cem. Concr. Compos.*, vol. 132, p. 104628, Sept. 2022, doi: 10.1016/j.cemconcomp.2022.104628.

[2]. L. Cui, X. Gao, M. Hang, and T. Chen, "Comparative Studies on Steel Corrosion Resistance of Different Inhibitors in Chloride Environment: The Effects of Multi-Functional Protective Film," *Appl. Sci.*, vol. 13, no. 7, p. 4446, Mar. 2023, doi: 10.3390/app13074446.

[3]. X. Wang *et al.*, "Performance of a Composite Inhibitor on Mild Steel in NaCl Solution: Imidazoline, Sodium Molybdate, and Sodium Dodecylbenzenesulfonate," *Coatings*, vol. 14, no. 6, p. 652, May 2024, doi: 10.3390/coatings14060652.

[4]. T. K. Rout and N. Bandyopadhyay, "Effect of molybdate coating for white rusting resistance on galvanized steel," *Anti-Corros. Methods Mater.*, vol. 54, no. 1, pp. 16–20, Jan. 2007, doi: 10.1108/00035590710717348.

[5]. R. Farahmand, B. Sohrabi, A. Ghaffarinejad, and M. R. Zamani Meymian, "Synergistic effect of molybdenum coating and SDS surfactant on corrosion inhibition of mild steel in presence of 3.5% NaCl," *Corros. Sci.*, vol. 136, pp. 393–401, May 2018, doi: 10.1016/j.corsci.2018.03.030.

[6]. M. A. Ahmed, S. Amin, and A. A. Mohamed, "Current and emerging trends of inorganic, organic and eco-friendly corrosion inhibitors," *RSC Adv.*, vol. 14, no. 43, pp. 31877–31920, 2024, doi: 10.1039/D4RA05662K.

[7]. Y. Liu, X. Guan, and J. Shi, "Synergistic inhibition of molybdate and phytate on chloride-induced corrosion of carbon steel in simulated concrete pore solutions," *Cem. Concr. Compos.*, vol. 145, p. 105366, Jan. 2024, doi: 10.1016/j.cemconcomp.2023.105366.

[8]. P. Xu *et al.*, "Influence of sulfate salt type on passive film of steel in simulated concrete pore solution," *Constr. Build. Mater.*, vol. 223, pp. 352–359, Oct. 2019, doi: 10.1016/j.conbuildmat.2019.06.209.

[9]. Y. Zhou and Y. Zuo, "The inhibitive mechanisms of nitrite and molybdate anions on initiation and propagation of pitting corrosion for mild steel in chloride solution," *Appl. Surf. Sci.*, vol. 353, pp. 924–932, Oct. 2015, doi: 10.1016/j.apsusc.2015.07.037.

[10]. H. Verbruggen, H. Terryn, and I. De Graeve, "Inhibitor evaluation in different simulated concrete pore solution for the protection of steel rebars," *Constr. Build. Mater.*, vol. 124, pp. 887–896, Oct. 2016, doi: 10.1016/j.conbuildmat.2016.07.115.

[11]. M. Wu and J. Shi, "Beneficial and detrimental impacts of molybdate on corrosion resistance of steels in alkaline concrete pore solution with high chloride contamination," *Corros. Sci.*, vol. 183, p. 109326, May 2021, doi: 10.1016/j.corsci.2021.109326.

[12]. S. M. Abd El Haleem, S. Abd El Wanees, E. E. Abd El Aal, and A. Diab, "Environmental factors affecting the corrosion behavior of reinforcing steel II. Role of some anions in the initiation and inhibition of pitting corrosion of steel in $Ca(OH)_2$ solutions," *Corros. Sci.*, vol. 52, no. 2, pp. 292–302, Feb. 2010, doi: 10.1016/j.corsci.2009.09.004.

[13]. Q. Fu, H. Zhou, Z. He, X. Zhao, and D. Niu, "Depassivation mechanism of steel bar in concrete under the condition of flowing composite chloride salt and sulfate attack," *Constr. Build. Mater.*, vol. 450, p. 138696, Nov. 2024, doi: 10.1016/j.conbuildmat.2024.138696.

[14]. L. Cáceres, T. Vargas, and L. Herrera, "Influence of pitting and iron oxide formation during corrosion of carbon steel in unbuffered NaCl solutions," *Corros. Sci.*, vol. 51, no. 5, pp. 971–978, May 2009, doi: 10.1016/j.corsci.2009.02.021.

[15]. J. Shi, M. Wu, and J. Ming, "Long-term corrosion resistance of reinforcing steel in alkali-activated slag mortar after exposure to marine environments," *Corros. Sci.*, vol. 179, p. 109175, Feb. 2021, doi: 10.1016/j.corsci.2020.109175.